Frequency Dependence Study of a Bias Field-Free Nano-Scale Oscillator

T. Windbacher, D. Osintsev, A. Makarov, H. Mahmoudi, V. Sverdlov, and S. Selberherr
Institute for Microelectronics, TU Wien, Gußhausstraße 27–29/E360, 1040 Wien, Austria
e-mail: {windbacher|osintsev|makarov|mahmoudi|sverdlov|selberherr}@iue.tuwien.ac.at

***Abstract*—Oscillators belong to the group of fundamental building blocks and are ubiquitous in modern electronics. Especially spin torque nano oscillators are very attractive as cost effective on-chip integrated microwave oscillators, due to their nano-scale size, frequency tunability, broad temperature operation range, and CMOS technology compatibility. Recently, we proposed a micromagnetic structure capable of operating as non-volatile flip flop as well as a spin torque nano oscillator. The structure consists of three anti-ferromagnetically coupled stacks (two for excitation A, B and one for readout Q) and a shared free magnetic layer. Micromagnetic simulations show a current regime, where the structure exhibits large, stable, and tunable in-plane oscillations in the GHz range without the need of an external magnetic field or an oscillating current. In this work the dependence of these oscillations on the shared free layer geometry at a fixed input current is studied. It is shown that the precessional frequency can be controlled by the dimensions of the shared free layer. Most efficient is to utilize the layer thickness to control the precessional frequency, but also changing the layer length can be exploited.**

Introduction

Oscillators represent fundamental building blocks in modern electronics. They are required in measurement, navigation, communication systems, etc. The periodicity of their output signals is exploited for clocking digital circuits, generating electromagnetic waves, as a reference source for system synchronization, and much more [1]. Spin torque nano oscillators are very appealing as cost effective on-chip integrated microwave oscillators due to their nano-scale size, frequency tunability, broad temperature operation range, and CMOS technology compatibility [2]. Spin torque nano oscillators are also the smallest known auto-oscillators and represent complex nonlinear dynamical systems. The current challenges for applying spin torque nano oscillators in real world applications lie in the simultaneous optimization of a variety of properties, including high frequency operation, frequency tunability, narrow spectral line width, large output power, operation without external magnetic fields as well as operation at low applied current densities [2], [3], [4], [5], [6], [7].

During our work on a non-volatile magnetic flip flop [8], [9], we found a current regime, where the structure exhibits tunable, large, and stable magnetiztions oscillations without the need for an external magnetic field or an oscillating current [10]. The structure consists of three anti-ferromagnetically coupled stacks (two for excitation A, B and one for readout Q) and a shared free magnetic layer, where the mode excitations take place (see Fig. 1). It is essential to understand the frequency dependence of an oscillator on its device geometry to enable the design of devices with specified frequencies and to handle device variability due to manufacturing. Therefore, this work investigates the spin torque nano-scale oscillator's frequency dependence on its geometry.

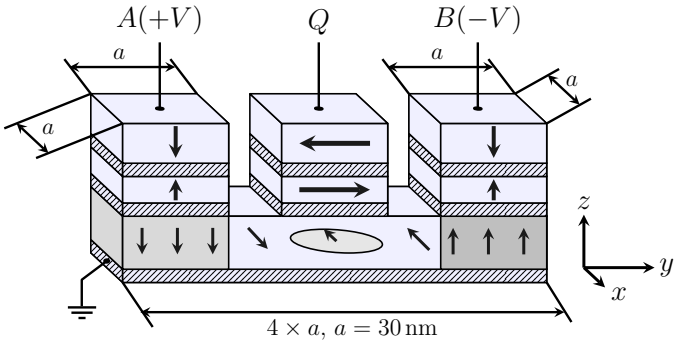

Fig. 1. The initial shared free layer is 30 nm wide, 120 nm long, and 3 nm thick. While changing only one of the free layers dimensions, the others are kept at their initial length. The input current was set constant to $10^{12}\,\mathrm{A/m^2}$ and an out-of-plane uni-axial anisotropy $K_1 = 10^5\,\mathrm{J/m^3}$ in the free layer was assumed.

Theory and Simulation Setup

Before explaining the employed models some basic assumptions and prerequisites must be elucidated. As stated before the non-volatile flip flop exhibits three fixed anti-ferromagnetically coupled polarizer stacks, two for excitation A, B with perpendicular (parallel to the z-axis) magnetization orientation and one for read out Q with in-plane magnetization orientation (see Fig. 1). The in-plane magnetization orientation is necessary to extract the larger in-plane component of the oscillations, instead of the much smaller vertical oscillations (see Fig. 2).

The shape anisotropie's easy axis is defined as an energetically favorable direction for the magnetization (local energy minima), while a hard axis describes a local energy maximum.

It is further assumed that due to the anti-ferromagnetic nature of the polarizer stacks their stray fields can be neglected. The shared free layer exhibits a constant out-of-plane uni-axial anisotropy described by K_1.

The free layer dimensions are varied independently, between $20\mathrm{nm}$ and $70\mathrm{nm}$ for the free layer width, between $90\mathrm{nm}$ and $150\mathrm{nm}$ for length, and between $1\mathrm{nm}$ and $5\mathrm{nm}$ for the layer thickness. The applied current density was fixed at

978-1-4799-5433-9/14/$31.00

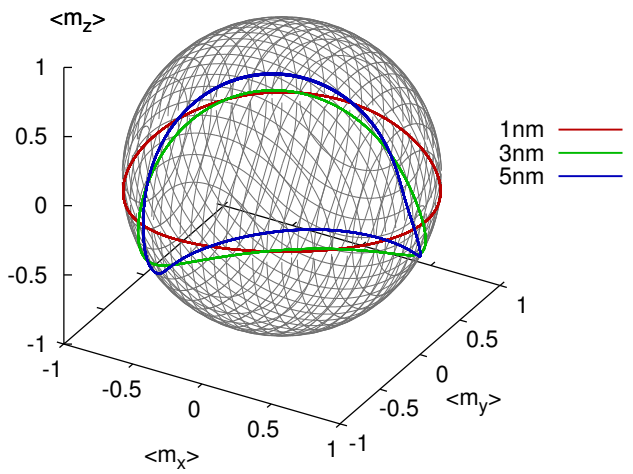

Fig. 2. Normalized pseudo macro spin magnetization oscillations of $<\vec{m}(t)>$ as a function of time. One can see the thinner the shared free layer, the weaker the net out-of-plane anisotropy and thus the more circular the precession path.

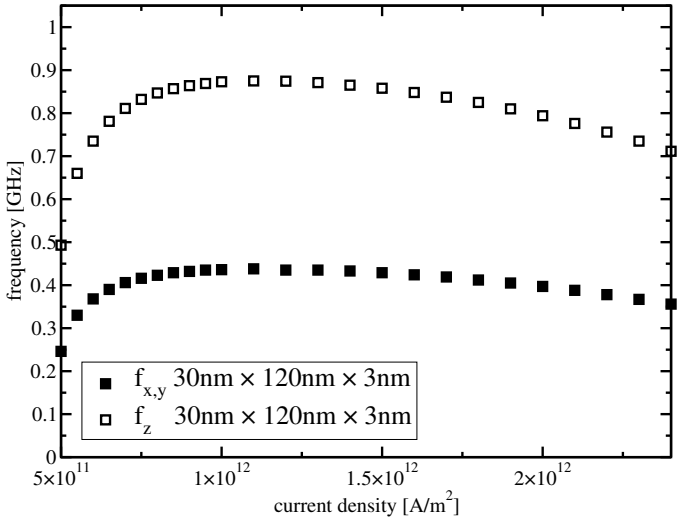

Fig. 3. Resonance frequencies in the xy-plane and z-direction as a function of the applied current density. The layer length, width, and thickness remain unchanged at 120 nm, 30 nm, and 3 nm, respectively.

Parameter	Value
Free layer length	$90 - 150\text{nm}$
Free layer width	$20 - 70\text{nm}$
Free layer thickness	$1 - 5\text{nm}$
Contact size a	$30\text{nm} \times \text{width}$
Magnetization saturation M_S	$4 \times 10^5 \text{A/m}$
Out-of-plane uni-axial anisotropy K_1	10^5J/m^3
Uniform exchange constant A_exch	$2 \times 10^{-11} \text{J/m}$
Polarization P	0.3
Non-magnetic layer	Cu
Gilbert gyromagnetic ratio γ	$2.211 \times 10^5 \text{m/As}$
Damping constant α	0.01
Non-adiabatic contribution ϵ'	0.1 [11]
current density J	10^{12}A/m^2
Fitting parameter Λ	2
Discretization length Δx, Δy	2nm
Discretization length Δz	$1 - 5\text{nm}$
Discretization time Δt	$2 \times 10^{-14} s$

TABLE I. SIMULATION PARAMETERS

10^{12}A/m^2 for each layer size. The devices' widths are oriented parallel to the x-axis, their lengths along the y-axis, and their thicknesses along the z-axis. The devices are powered by two synchronously applied currents.

Assuming a grounded metal layer at the bottom of the free layer and a positive voltage applied to one of the contacts (A, B, or Q) a current flow from the contacts, through the free layer towards the bottom contact will be induced (against the z-axis). This current flow is defined as the positive current direction. At the same time electrons will flow in the opposite direction (positive z-axis).

If a positive current is applied to one of the input stacks A or B, electrons will flow from the shared free layer to the polarizer stack. Electrons featuring a magnetic moment parallel to the polarizer stack's magnetization orientation can enter easily, while non-aligned electrons get their spin orientation aligned with the magnetization. Their spins relax to the local magnetization orientation and cause a spin torque which drives precessional motions of the free layer magnetization under the contact. The precessional motions couple through magnetic exchange to the rest of the free layer and start to excite precessional motions in the whole layer. The precessional motions build up, until they pass the energy barrier separating its two stable states eventually and relax fast into the other stable state.

If now two currents with identical amplitude but opposing polarities are applied, one acting torque tries to align the free layer magnetization parallel to the z-axis, while the other one always strives to push it into the opposite anti-parallel position. Provided that the two currents are strong enough to overcome the damping of the free layer, the magnetization in the free layer can not relax and is pushed continously back and forth between the input stacks A and B. These oscillations are developed without applying an external magnetic field otherwise needed to achieve precession as discussed in earlier proposed structures [12], [13], [14]. Because of the negligible stray fields from the polarizers the precessions are not localized under the fixed layers, as in [12], [13], [14]. Instead the entire layer carries out the precessional movement [10].

The simulation parameters were chosen identical to the simulation parameters from [8] to keep the simulation results comparable. All relevant parameters are summarized in Tab. I.

Instead of tuning the input current and keeping the aspect ratio constant, we varied, the length, width, and thickness of the shared free layer independently. The respective structures are modeled by the Landau-Lifshitz-Gilbert equation [15].

$$\frac{d\vec{m}}{dt} = \gamma \left(-\vec{m} \times \vec{H}_\text{eff} + \alpha \left(\vec{m} \times \frac{d\vec{m}}{dt} \right) + \vec{T} \right), \qquad (1)$$

$\vec{m}$ denotes the reduced magnetization, γ the Gilbert gyromagnetic ratio, α the dimensionless damping constant, and $\vec{H}_\text{eff}$ the effective field in A/m. The last term in (1) describes the spin transfer torque $\vec{T}$ arising from the polarized electrons acting on the local magnetization and is modeled with the following

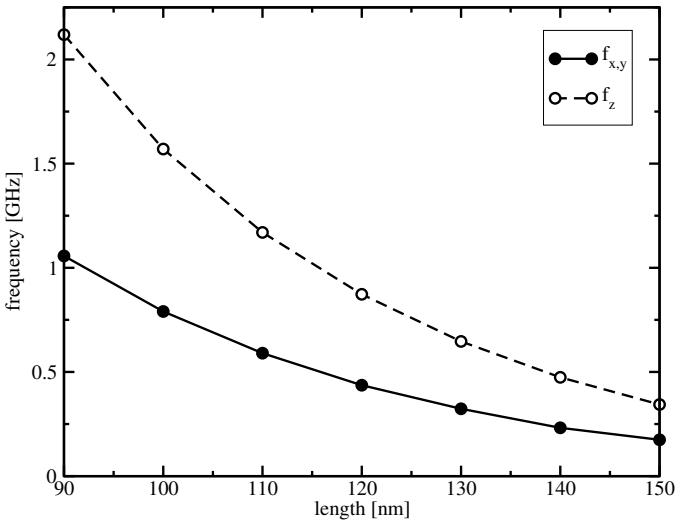

Fig. 4. Resonance frequencies in the xy-plane and z-direction as a function of the shared free layer length. The layer width and thickness remain unchanged at 30 nm and 3 nm, respectively.

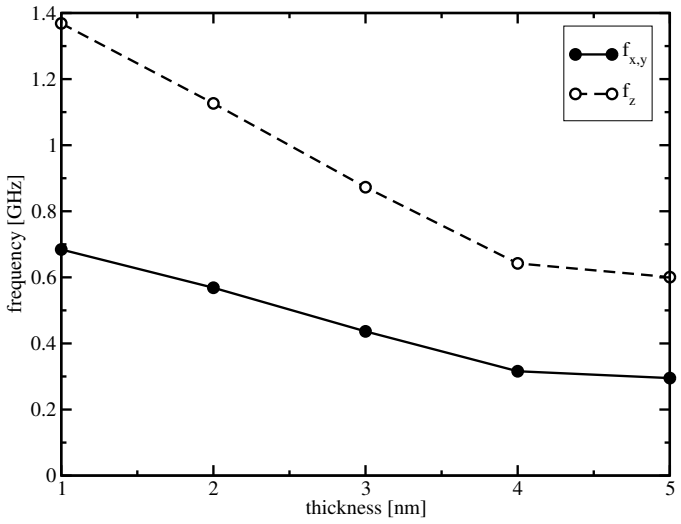

Fig. 5. Resonance frequencies in the xy-plane and z-direction as a function of the shared free layer thickness. The layer length and width remain unchanged at 120 nm and 30 nm, respectively.

spin transfer torque model [16]:

$$\vec{T} = \frac{\hbar}{\mu_0 e}\frac{J}{l M_S}\frac{P\Lambda^2}{(\Lambda^2+1)+(\Lambda^2-1)\,\vec{m}\cdot\vec{p}} \cdot \cdot (\vec{m}\times\vec{p}\times\vec{m} - \epsilon'\vec{m}\times\vec{p}) \quad . \tag{2}$$

$\hbar$ denotes the Planck constant, μ_0 the permeability of vacuum, e the electron charge, J the applied current density, l the free layer thickness, M_S the magnetization saturation, P the polarization, $\vec{p}$ the unit polarization direction of the polarized current, and Λ is a fitting parameter handling non-idealities.

Furthermore, $\vec{H}_\mathrm{eff}$ is calculated from the functional derivative of the free energy density containing uni-axial anisotropy, exchange, and demagnetization contributions [15].

Results

Starting point is a shared free layer with 30 nm width, 120 nm length, and 3 nm thickness (see Fig. 1 and Fig. 3). Fig. 4 shows that increasing the layers' length decreases the precession frequency. This is consistent with geometrically controlled resonance conditions, where a longer oscillation path leads to a lower frequency, due to the back and forth motion of a phase wave between the two excitation regions A and B. The longer the path between A and B, the more time it takes the phase wave to commute ($\Delta f/\Delta l \approx -14.7\,\mathrm{MHz/nm}$).

Looking at Fig. 5 shows that with increasing layer thickness the precessional frequency drops down ($\Delta f/\Delta z \approx -780\,\mathrm{MHz/nm}$). The observed behavior is due to the interplay of two counteracting anisotropies in the shared free layer. One is the out-of-plane uniaxial anisotropy K_1, which was assumed to be constant, and the other one is the shape anisotropy. The shape anisotropy strongly depends on the length ratios of the shared free layer [17]. Reducing the layer thickness leads to an increase in the shape anisotropy hard axis along z but at the same time to a weaker easy (y-direction) and hard axis (x-direction) in the xy-plane resulting in an increase of the precession frequency [18] (cf. Fig. 2).

On the other hand changing the layer width increases the frequency slightly (see Fig. 6, $\Delta f/\Delta w \approx 1.75\,\mathrm{MHz/nm}$). This at first seems contradictory in comparison to Fig. 4 and Fig. 5. However, increasing the layer width decreases the in-plane hard axis and easy axis. At the same time the contact width is defined the same as the free layer width. Therefore, increasing the width is correlated to increasing linearly the applied current as well as the shared free layer volume. For a high device width the shape anisotropies start to saturate and the linear volume increase (more total magnetic momentum to excite) is compensated by the linearly growing applied current, thus leading to a saturation in the precession frequency for increasing layer width.

Fig. 2 illustrates the averaged total magnetization $<\vec{m}>$ as a function of time and shared free layer thickness. The precessional motion consists of a superposition of an in-plane rotation and an out-of-plane oscillation. It also explains why the in-plane and the out-of-plane precession frequency components are coupled by a factor of 2, since for a closed precessional orbit the z-component makes two oscillations for the whole loop in the xy-plane. The decreasing out-of-plane oscillations (decreasing curvature) of the orbits, when the free layer thickness is reduced, stems from increasing the out-of-plane shape anisotropy, which opposes the out-of-plane uniaxial anisotropy K_1. The resulting net anisotropy along the z-axis becomes smaller and makes the growing in-plane hard and easy axes energetically more favorable.

Discussion

While variations in the layer width influence the precession frequency by a factor of 10 less than length variations, changes in the layer thickness lead to a huge frequency shift. Reducing

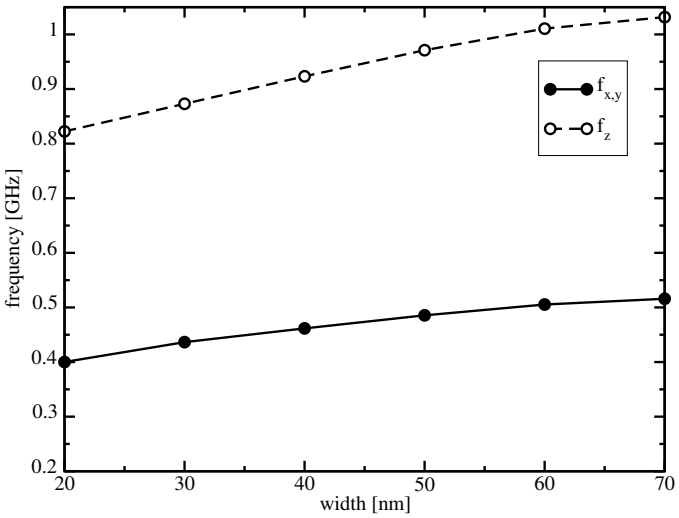

Fig. 6. Resonance frequencies in the xy-plane and z-direction as a function of the shared free layer width. The layer length and thickness remain unchanged at 120 nm and 3 nm, respectively.

the layer thickness leads to an increase of the shape anisotropy along the z direction. This contribution opposes and weakens the out-of-plane anisotropy of the free layer and leads to a pronounced shift to in-plane oscillations for thinner free layers (cf. Fig. 2 and [18]).

On the other hand keeping the length and the thickness constant while decreasing the width of the free layer leads to a reduction in the precession frequency. Here, the increase of the hard axis strength along the x-axis for smaller width causes the frequency reduction. In the case of changing the thickness of the free layer the situation is not so straightforward (cf. Fig. 5). According to [17] decreasing the layer thickness leads to an increase of the shape anisotropy hard axis pointing out of plane. At the same time the assumed perpendicular anisotropy is kept constant. Since these two contributions oppose each other, the resulting net magnetic easy axis along the z-axis becomes smaller. This makes it energetically favorable for the magnetization to rotate in the xy-plane and hence the frequency increases.

Conclusion

It has been shown that the precessional frequency can be controlled by the dimensions of the shared free layer. It is most efficient to change the layer thickness to control the precessional frequency, but also changing the layer length can be exploited.

Acknowledgment

This research is supported by the European Research Council through the Grant #247056 MOSILSPIN.

References

[1] U. Tietze and C. Schenk, *Electronic Circuits – Handbook for Design and Applications*, 2nd ed. Springer, 2008, no. 12.

[2] Z. Zeng, G. Finocchio, B. Zhang, P. K. Amiri, J. A. Katine, I. N. Krivorotov, Y. Huai, J. Langer, B. Azzerboni, K. L. Wang, and H. Jiang, "Ultralow-Current-Density and Bias-Field-Free Spin-Transfer Nano-Oscillator," *Sci. Rep.*, vol. 3, pp. 1–5, Mar. 2013. [Online]. Available: http://dx.doi.org/10.1038/srep01426

[3] G. Finocchio, A. Prattella, G. Consolo, E. Martinez, A. Giordano, and B. Azzerboni, "Hysteretic Spin-Wave Excitation in Spin-Torque Oscillators as a Function of the In-Plane Field Angle: A Micromagnetic Description," *J.Appl.Phys.*, vol. 110, no. 12, 2011.

[4] K. Y. Guslienko, G. R. Aranda, and J. Gonzalez, "Spin Torque and Critical Currents for Magnetic Vortex Nano-Oscillator in Nanopillars," *Journal of Physics: Conference Series*, vol. 292, no. 1, p. 012006, 2011.

[5] G. Finocchio, O. Ozatay, L. Torres, R. A. Buhrman, D. C. Ralph, and B. Azzerboni, "Spin-Torque-Induced Rotational Dynamics of a Magnetic Vortex Dipole," *Physical Review B*, vol. 78, p. 174408, 2008.

[6] L. Liu, C.-F. Pai, Y. Li, H. W. Tseng, D. C. Ralph, and R. A. Buhrman, "Spin-Torque Switching with the Giant Spin Hall Effect of Tantalum," *Science*, vol. 336, no. 6081, pp. 555–558, 2012.

[7] L. Liu, C.-F. Pai, D. C. Ralph, and R. A. Buhrman, "Magnetic Oscillations Driven by the Spin Hall Effect in 3-Terminal Magnetic Tunnel Junction Devices," *Physical Review Letters*, vol. 109, p. 186602, 2012.

[8] T. Windbacher, H. Mahmoudi, V. Sverdlov, and S. Selberherr, "Rigorous Simulation Study of a Novel Non-Volatile Magnetic Flip Flop," in *Proc. of the SISPAD*, 2013, pp. 368–371.

[9] ——, "Spin Torque Magnetic Integrated Circuit," EU Patent EP13 161 375, Mar. 27, 2013, pending.

[10] T. Windbacher, A. Makarov, H. Mahmoudi, V. Sverdlov, and S. Selberherr, "Novel Bias-Field-Free Spin Transfer Oscillator," vol. 115, pp. C901–1 – C901–3, 2014.

[11] A. V. Khvalkovskiy, K. A. Zvezdin, Y. V. Gorbunov, V. Cros, J. Grollier, A. Fert, and A. K. Zvezdin, "High Domain Wall Velocities Due to Spin Currents Perpendicular to the Plane," *Physical Review Letters*, vol. 102, p. 067206, 2009.

[12] C. Boone, J. A. Katine, J. R. Childress, J. Zhu, X. Cheng, and I. N. Krivorotov, "Experimental Test of an Analytical Theory of Spin-Torque-Oscillator Dynamics," *Physical Review B*, vol. 79, p. 140404, 2009.

[13] G. Finocchio, N. Maugeri, L. Torres, and B. Azzerboni, "Domain Wall Dynamics Driven by a Localized Injection of a Spin-Polarized Current," *Magnetics, IEEE Transactions on*, vol. 46, no. 6, pp. 1523–1526, 2010.

[14] D. V. Berkov, C. T. Boone, and I. N. Krivorotov, "Micromagnetic Simulations of Magnetization Dynamics in a Nanowire Induced by a Spin-Polarized Current Injected via a Point Contact," *Physical Review B*, vol. 83, p. 054420, 2011. [Online]. Available: http://link.aps.org/doi/10.1103/PhysRevB.83.054420

[15] H. Kronmüller, *Handbook of Magnetism and Advanced Magnetic Materials*. John Wiley & Sons, Ltd, 2007, ch. General Micromagnetic Theory.

[16] J. Xiao, A. Zangwill, and M. D. Stiles, "Boltzmann Test of Slonczewski's Theory of Spin-Transfer Torque," *Physical Review B*, vol. 70, p. 172405, 2004.

[17] J. A.Osborn, "Demagnetization Factors of the General Ellipsoid," *Physical Review*, vol. 67, no. 11,12, pp. 351–357, 1945.

[18] A. Aharoni, "Demagnetizing Factors for Rectangular Ferromagnetic Prisms," *J.Appl.Phys.*, vol. 83, no. 6, pp. 3432–3434, 1998.